

RESEARCH ARTICLE

Structural connectivity of the human massa intermedia: A probabilistic tractography study

Alireza Borghei¹ | Irem Kapucu² | Robert Dawe² | Mehmet Kocak³ | Sepehr Sani¹ 

¹Department of Neurosurgery, Rush University Medical Center, Chicago, Illinois

²Rush Alzheimer's Disease Center, Johnston R Bowman Health Center, Chicago, Illinois

³Department of Radiology, Rush University Medical Center, Chicago, Illinois

Correspondence

Sepehr Sani, Department of Neurosurgery, Rush University Medical Center, 1725 W. Harrison St, Ste 855, Chicago, IL 60612. Email: sepehr_sani2@rush.edu

Funding information

McDonnell Center for Systems Neuroscience; NIH Blueprint for Neuroscience Research; NIH Institutes

Abstract

The role of massa intermedia (MI) is poorly understood in humans. Recent studies suggest its presence may play a role in normal human neurocognitive function while prior studies have shown the absence of MI correlated with psychiatric disorders. There is growing evidence that MI is likely a midline white matter conduit, responsible for interhemispheric connectivity, similar to other midline commissures. MI presence was identified in an unrelated sample using the Human Connectome Project database. MI structural connectivity maps were created and gray matter target regions were identified using probabilistic tractography of the whole brain. Probabilistic tractography revealed an extensive network of connections between MI and limbic, frontal and temporal lobes as well as insula and pericalcarine cortices. Women compared to men had stronger connectivity via their MI. The presented results support the role of MI as a midline commissure with strong connectivity to the amygdala, hippocampus, and entorhinal cortex.

KEYWORDS

Human Connectome Project, interthalamic adhesion, massa intermedia, probabilistic Tractography, structural connectivity

1 | INTRODUCTION

The massa intermedia (MI), otherwise known as the interthalamic adhesion, is a midline structure that connects the two thalami. It was originally described by Giovanni Battista Morgagni in 1719 (Olry & Haines, 2005). While this structure is relatively large in lower mammals, its size is more variable in higher order primates. In some humans, MI is entirely absent altogether (Edinger, 1904; Fortuyn & Stefens, 1951; Malobabic, Puskas, & Vujaskovic, 1990; Rioch, 1931). For that reason, Frauceiger (1959) described the MI as an ancestral remnant of lower mammals and considered its role as insignificant in humans, despite the evolutionary preservation of it across mammalian species (Rioch, 1931). Since then, an increasing body of literature has

shed light on MI as a midline commissure, possibly serving a similar role as the corpus callosum, anterior commissure (AC), and posterior commissure (PC) (Clark & Russell, 1939; Fortuyn & Stefens, 1951; Hiyoshi & Wada, 1988b; Jin, Kalimo, & Panula, 2002; Morel, Magnin, & Jeanmonod, 1997; Wada, Sato, & Corcoran, 1974).

In humans, MI is absent in 2.3–31.7% of brains (Carpenter & Sutin, 1983; de Macedo, 1889; Malobabic, Puskas, & Blagotic, 1987; Rabl, 1958; Samra & Cooper, 1968; Sen, Ulubay, Ozeksi, Sargon, & Tascioglu, 2005; Takahashi et al., 2008). Cadaveric studies as well as in vivo neuroimaging studies using magnetic resonance imaging (MRI) have reported conflicting results on age and sex predilection of MI presence and size (Damle et al., 2017; Matsumoto, 1937; Mohammadi, Hosseini, & Golalipour, 2008; Morel, 1947; Nopoulos,

This is an open access article under the terms of the Creative Commons Attribution-NonCommercial-NoDerivs License, which permits use and distribution in any medium, provided the original work is properly cited, the use is non-commercial and no modifications or adaptations are made.

© 2020 The Authors. *Human Brain Mapping* published by Wiley Periodicals LLC.

Rideout, Crespo-Facorro, & Andreasen, 2001; Rabl, 1958), potentially owing to variable image acquisition techniques and inconsistent identification and measurement paradigms. A cadaveric study by Allen and Gorski (1991) revealed that MI was present in 78% of females and 68% of males and when present, it was 76% larger in females than in males. This is consistent with an MRI study that also noted larger MI size in healthy women compared to age-matched men (Shimizu et al., 2008). In addition, a recent study (Damle et al., 2017) reported higher prevalence of MI among females and an age-related decrease in size of MI.

Several studies have attempted to correlate the inconsistent presence and age and sex predilection of MI with psychiatric diagnoses and cognitive processes (Borghesi, Cothran, Brahimaj, & Sani, 2020; Ceyhan, Adapinar, Aksaray, Ozdemir, & Colak, 2008; Damle et al., 2017; Takahashi, Suzuki, Zhou, et al., 2008; Trzesniak et al., 2011). Cheryan, Romo, Godeheu, and Glowinski (1984) demonstrated a possible role of MI in dopaminergic regulation of the limbic system and Romo, Cheryan, Godeheu, and Glowinski (1984) described a similar role for MI in the substantia nigra and caudate nucleus of the cat. In male humans suffering from schizophrenia spectrum disorder (SSD), a disease partly characterized by dopaminergic dysregulation (Grace, 2016), MI is more likely to be absent compared to female patients (absent in 36.8 vs. 8.8%) (Takahashi, Suzuki, Zhou, et al., 2008). SSD patients are twice as likely as healthy controls to lack MI (Trzesniak et al., 2011). More recently, MI size differences have been associated with neuropsychological measures of attention functioning in healthy females (Damle et al., 2017). In another recent investigation, presence of MI was identified as a mediator between increased score in attention task (flanker test) and decreased feeling of loneliness. MI size was also found to mediate the relation between age and scores of Continuous Performance Test-Identical Pairs "CPT-IP" in healthy female participants (Borghesi et al., 2020). MI has also been reported as more prevalent and bigger in female participants (Borghesi et al., 2020). This is consistent with a prior study noting smaller average MI size in male subjects when compared to female subjects (Trzesniak et al., 2016). Collectively, this body of evidence supports the notion that MI is an interhemispheric commissural pathway, interconnecting the limbic and cognitive processing networks with gender differences in prevalence and size.

Computational neuroimaging techniques have been used to better understand the anatomical connectivity of MI (Damle et al., 2017; Kochanski, Dawe, Kocak, & Sani, 2018). Probabilistic tractography techniques offer the advantage of studying small fiber tracks across a large number of brains for validity and reproducibility. Damle et al. (2017), in light of earlier studies (Kamali, Kramer, & Hasan, 2010; Spalletta, Fagioli, Caltagirone, & Piras, 2013), have demonstrated MI fibers traveling through the anterior thalamic radiation to the prefrontal cortex. In a study using diffusion MR in pediatric brains with malformation, Poretti and his colleagues demonstrated attempted interhemispheric connections through the region of MI in a case of agenesis of corpus callosum (Poretti, Meoded, Rossi, Raybaud, & Huisman, 2013). Our group has recently reported (Kochanski et al., 2018) the presence of a contralateral stria medullaris pathway

through the MI, connecting the prefrontal cortex to the contralateral habenular nuclei. The fibers travel in the anterior limb of internal capsule, entering the thalamus presumably via the anterior thalamic radiation to cross contralaterally through MI, ending in the lateral habenula nucleus.

Despite accumulating evidence suggesting MI as a commissural pathway, a study of the entire structural connectivity of MI is lacking. The objective of this study was to use the large human neuroimaging repository of the Human Connectome Project and probabilistic tractography techniques to perform a comprehensive analysis of the connectivity patterns of fibers crossing MI. The aims of our study were to identify the prevalence of brains with MI, and when present, identify the most commonly visualized fiber tracks across MI.

2 | MATERIAL AND METHODS

2.1 | Subjects

We utilized a 100-subject subset of the 1,200-subject dataset of the Human Connectome Project (Van Essen et al., 2013). This cohort, unlike the main HCP subjects, was designed to randomly include non-related (i.e., not belonging to the same family) participants to eliminate the confounding effects of shared genetic profiles of siblings. This sub-cohort is readily available and free to download ("Human Connectome Project,"). Subjects were healthy young humans between 22 and 35 years old. This age range was originally chosen by HCP investigators to minimize the effect of age on neurodevelopmental and/or neurodegenerative changes associated with younger and older humans respectively. Being healthy was defined in a way to include people from a wide range of differences in regards to environmental factors including social, economic, ethnic and ethnologic. All participants had no history of definitive psychiatric and neurologic diseases (Van Essen et al., 2012).

2.2 | Image acquisition

MR imaging of all subjects was carried out using an HCP-customized 3T Siemens Skyra with a 32-channel head coil (Van Essen et al., 2012). A 3D MPRAGE sequence was used to acquire two T1-weighted (T1W) volumes with a field of view of 224 mm and resolution of 0.7 mm isotropic (TR = 2,400 ms, TE = 2.14 ms, TI = 1,000 ms, flip angle = 8°) (Glasser et al., 2013). To reduce eddy current induced distortion, reversed phase-encoding was used in HCP diffusion weighted (DW) image acquisition. DW data were acquired via 3 pairs of left-to-right and right-to-left phase encoding acquisitions each consisting of 90 diffusion directions and $b = 0$. Each run had three shells consisting of diffusion weightings of $b = 1,000$ s/mm², $b = 2,000$ s/mm² and $b = 3,000$ s/mm². Use of multiple shells is shown to improve both fiber orientation and crossing fiber identification by 34 and 21% respectively when compared to single shell diffusion MR (Sotiropoulos et al., 2013). A partial Fourier factor of 6/8

resulted in an echo train length of 84 ms and echo time (TE) of 89.5 ms. Resolution was 1.25 mm isotropic. Additional details of the MRI protocol and rationale can be found in (Sotiropoulos et al., 2013).

2.3 | Pre-processing

Detailed processing steps have been described previously (Glasser et al., 2013). In summary, T1-weighted images were corrected for gradient nonlinearity using *gradient_nonlin_unwarp* available via FreeSurfer (version 5.2). These distortion-corrected images were aligned rigidly to MNI space (Montreal Neurological Institute and Hospital atlas). Echo planar imaging (EPI) distortion correction of the DW images was performed with FSL version 5 TOPUP tool using the six available reversed-phase DW images available for each diffusion direction (Andersson, Skare, & Ashburner, 2003). The estimated field of distortion was then used along with inhomogeneity field caused by eddy current as well as head motion of each volume for correction using a Gaussian process model (Andersson et al., 2012).

2.4 | MI identification

Anatomical T1 weighted scans were AC-PC aligned with the MNI-152 atlas to allow (Sotiropoulos et al., 2013) creation of regions of interest (ROI) and calculate further measurements of ROIs. Four raters independently identified subjects with no MI. Raters were blind to gender, age and health status of the subjects as well as other raters' responses. Axial and coronal T1W images corresponding to the third ventricle were examined. If a midline interthalamic connection was noted, it was subsequently confirmed using a midline sagittal view by noting circumferential cerebrospinal fluid (CSF) low intensity signal around the MI (Figure 1). Subsequently, the maximum dorsoventral

and cephalocaudal diameter of each MI was measured using the measurement tool available in *freeview* on the corresponding axial and coronal slices, respectively.

2.5 | MI seed masking

A binary mask was created on T1W AC-PC aligned NIFTI images using the *fsleyes* GUI (graphical user interface). For each brain with an MI, the mid-sagittal plane of MI was selected by navigating the transverse view. Then all voxels representing MI on sagittal view surrounded by CSF signal were selected as the MI mask. To increase the number of seed mask's voxels, the single-voxel-width ROI was augmented with a single-voxel-width plane in the immediately adjacent left and right sagittal slices. This step was done to address possible omission of diffusion data due to higher resolution of the anatomical images and small width of a single-voxel seed mask (e.g., DW images have 1.25 mm isotropic while T1W anatomical scan have 0.7 mm isotropic).

2.6 | Tractography

To our knowledge there is no prior human study of the structural connectivity of MI. Therefore, we designed a three stage tractography approach to determine probable gray matter (GM) destination of fibers crossing through MI. First, we manually explored each individual MI's probabilistic tractogram to identify possible cortical and subcortical GM target regions. In the second stage, probabilistic tractography was performed with MI as the seed mask and each GM target region, identified in the previous step, as the waypoint and termination mask. Probabilistic tractography was performed using *probtrackx2* tool of FMRIB Software Library, *FSL* (Behrens et al., 2003; Behrens, Berg, Jbabdi, Rushworth, & Woolrich, 2007). In the third stage, to verify the

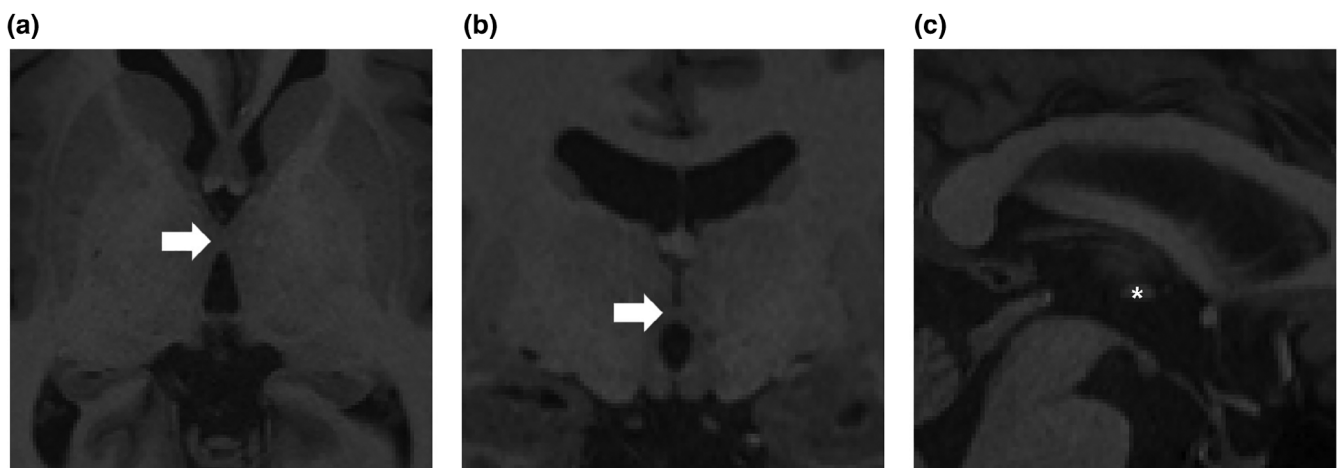


FIGURE 1 Identification of massa intermedia (MI). T1 weighted images showing (a) axial, (b) coronal and (c) sagittal views of MI. The axial view was navigated to choose the mid-sagittal plane. If a midline interthalamic connection was noted, it was subsequently confirmed on the coronal views followed by midline sagittal views where presence of circumferential cerebrospinal fluid (CSF) low intensity signal around the MI was verified. The arrows and the asterisk demonstrate location of MI

identified target regions originated in the contralateral hemisphere and crossed MI, ipsilateral thalami were seeded and contralateral GM targets that were identified in stage two were used as waypoints to verify passage of fibers interhemispherically through MI. Figure 2 depicts these steps which are described in detail below. Due to lack of prior studies on human MI structural connectivity we used a two-stage process, referred to here as “Exploratory Target Selection” and “ROI tractography.”

2.7 | Exploratory target selection

In the first stage, whole brain probabilistic tractography results were manually inspected and consistent GM targets having connection with MI across all subjects were selected. In this stage, the MI mask was introduced as a seed mask and probtrackx2 was run with 5,000 samples per seed voxel with no specified waypoint or termination masks. We used default values for curvature thresholds, maximum number of steps and step length, which were 0.2, 2,000 and 0.5 respectively. Manual inspection of each output track was

then performed to look for GM target regions connected to MI. The dynamic range of visualization was gradually reduced while GM targets, defined by *freesurfer* parcellated image available in HCP repository, were identified in each brain. GM targets with connectivity to MI that were seen across all subjects were selected for the next stage.

2.8 | ROI Tractography

In the second stage, previously identified GM target ROIs were extracted and binarized for each brain. The *freesurfer* parcellated anatomical image was used for creating target ROIs. Then probtrackx2 was run for each individual, with MI as seed mask and each GM target as a waypoint mask as well as a termination mask in order to include the tracts which entered the GM target and exclude the exiting tracts. Default values were again used for probtrackx2 tool. Number of successful probabilistic streamlines connecting MI to each GM target were divided by the product of the number of target ROI's voxels and the corresponding MI number of seed voxels to get to a “normalized

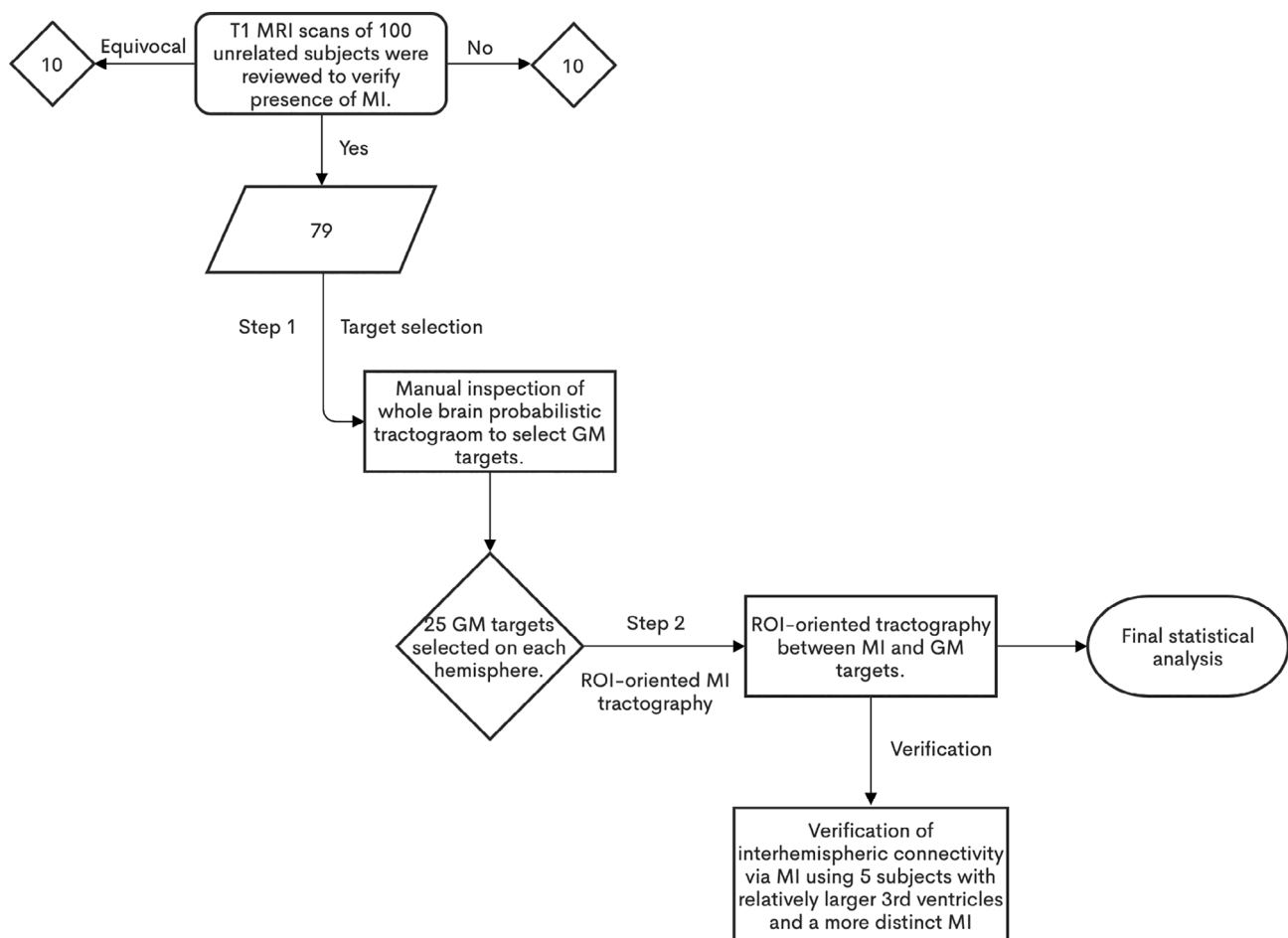


FIGURE 2 Flowchart depicting the steps taken to identify structural connectivity of massa intermedia (MI). Seventy-nine brains with MI undergone whole-brain tractography in Step 1 to identify gray matter areas with connection to MI. In Step 2, regions of interest (ROI)-based tractography yielded quantitative results. Finally, interhemispheric connectivity via MI was verified using tractography of a subset of subjects with a distinct MI seen on the T1 scans

measure” for comparison between different-sized GM target regions as well as different number of MI mask’s voxels.

The calculated normalized measure of connectivity (MC) of each tract t in individual i where W_{it} is the number of successful probabilistic streamline (way) between S_j number of MI seed voxels and G_{it} number of gray mater target mask’s voxels was calculated using the following equation:

$$M_{it} = \frac{W_{it}}{S_j \times G_{it}} \quad (1)$$

As the calculated measure was quite smaller than 1 in many cases, it was multiplied by 100,000 for ease of comparison.

2.9 | Verification of interhemispheric connectivity via MI

To verify the true passage of fibers via MI, five brains with large third ventricles (4.082 ± 0.33 mm) with distinct a MI were selected. For each brain, the ipsilateral thalamus was set as the seed mask. Corpus callosum, brainstem, AC and PC and the remainder of the ipsilateral hemisphere were selected as exclusion masks. Seven most connected GM regions (found in the second stage of analysis) from the contralateral hemisphere were then selected as the waypoint masks. Default values were left unchanged for probabilistic tractography with probtrackx2 as outlined earlier in the methods (see Appendix S1 for a more detailed explanation).

2.10 | Statistical analysis

Student t test was used for normally distributed data. To investigate gender difference in MI connectivity, subjects were grouped according to their gender. Mann–Whitney U test was then used to compare MI connectivity with GM regions of female versus male subjects using the calculated MC. A p value smaller than .05 was set as significant. Bonferroni method was utilized to control for multiple comparison when appropriate. Statistical analysis was performed using SPSS (IBM Corp. Armonk, NY).

3 | RESULTS

All raters agreed on the absence of MI in 11 out of 100. Ten brains were excluded due to inability to confirm either presence or absence of MI among all raters. Fleiss’s kappa coefficient (Fleiss & Cohen, 1973) for inter-rater correlation was .61 ($p < .001$).

Out of the total of 79 brains included in the final analysis 53 were female. Five female participants had no MI versus 6 male individuals with no MI. The mean cephalocaudal MI diameter was 11.42 mm (minimum: 7.68 mm, maximum: 15.02 mm, $SD = 1.30$) and the mean dorsoventral diameter was 16.04 mm (minimum: 10.7 mm, maximum: 21.88 mm,

TABLE 1 Mean cephalocaudal and dorsoventral dimension of MI ($n = 79$) in millimeters

	Mean (SD)		p value
	Female ($n = 48$)	Male ($n = 31$)	
Cephalocaudal dimension	11.61 (1.33)	11.11 (1.48)	.124
Dorsoventral dimension	16.25 (1.77)	15.7 (2.01)	.209

Abbreviation: MI, massa intermedia.

$SD = 1.87$) (Table 1). No significant correlation was found between gender and either cephalocaudal or dorsoventral diameters of MI.

Manual inspection of local connectivity of MI in all subjects revealed 25 GM targets on each hemisphere as shown in Table 2. Figure 3 shows histograms of MI connectivity with all 25 targets in each hemisphere sorted from high to low based on the calculated MC (Equation 1). A wide anatomical distribution of connectivity was noted. As seen in Figure 3, the amygdala, hippocampus, entorhinal cortex, insula, medial and lateral orbitofrontal cortices, pericalcarine cortex and cuneus of the occipital lobe were among the most connected GM regions to MI.

There were significant differences among these GM targets’ connectedness to MI in both hemispheres (Friedman’s analysis of variance, $p < .001$). Pairwise comparisons in the left hemisphere were significant except for entorhinal versus hippocampus and medial orbitofrontal, insula versus pericalcarine and cuneus, and cuneus versus pericalcarine. On the right, no significance was found when comparing entorhinal versus hippocampus and insula, cuneus versus pericalcarine, medial and lateral orbitofrontal cortices and lateral orbitofrontal versus medial orbitofrontal cortex. Additional details are provided in Appendix S1.

Right hemisphere targets with highest connectivity measures to MI had greater values than left hemisphere targets except for medial orbitofrontal cortex (Wilcoxon, $p = .280$ and $< .001$ for the latter and the rest of GM areas respectively). However, when corrected for handedness, only right-handed subjects showed interhemispheric difference (see Appendix S2 for details).

Analysis of sexual dimorphism revealed statistical significance among local connectivity measures tested by Mann–Whitney U nonparametric test (Table 2). Bonferroni adjusted p values were calculated. In the right hemisphere, inferior and superior parietal, lateral occipital, lateral orbitofrontal, lingual, pericalcarine cortices as well as pre-central and precuneus had significantly higher connectivity with MI in female subjects than the males. Female subjects also showed a higher MI connectivity to the left cerebellum, superior parietal, pre-central and precuneus cortices.

Tractography of five brains with large third ventricles further revealed passage of fibers from ipsilateral thalamus to the seven most MI-connected GM regions on the contralateral hemisphere. Figure 4 shows tractography of the left thalamus of a single participant. Averaged, normalized and aligned results of all five brains are delineated in Appendix S3.

TABLE 2 Structural connectivity of MI to various gray matter foci

Target	Right hemisphere			Left hemisphere		
	Mean (SD)		p Value ^a	Mean (SD)		p Value ^a
	Female	Male		Female	Male	
Amygdala	7,699.2 (3,832.77)	5,146.7 (3,177.69)	.1	1,077.3 (792.31)	1,216.1 (1,233.57)	1
Cerebellum	32.6 (24.5)	30.2 (36.92)	1	27 (18.76)	14.3 (10.86)	.05
Cuneus	137.8 (116.38)	98.4 (97.38)	1	44.4 (22.87)	40.2 (44.32)	.2
Entorhinal	1,829.7 (1,404.21)	1,240.7 (1,219.04)	.8	171.5 (153.31)	317.1 (512.15)	1
Fusiform	114.3 (109.85)	81.4 (73.35)	1	20.8 (15.55)	22.6 (24.47)	1
Hippocampus	1,809.3 (821.22)	1,412.8 (730.71)	1	355.8 (265.51)	404.4 (397.33)	1
Inferior parietal	25.3 (18.51)	10.7 (8)	<.001	9.8 (6.47)	6.2 (4.59)	.15
Inferior temporal	105.2 (92.24)	62.5 (51.22)	.6	12.1 (8.37)	11.6 (10.15)	1
Insula	934.3 (690.57)	700.7 (713.42)	1	73.3 (86.77)	92.5 (136.01)	1
Lateral occipital	104.3 (62.64)	60.7 (41.97)	<.001	29 (20.3)	25.8 (27.19)	1
Lateral orbitofrontal	215.3 (325.03)	207.1 (547.02)	<.001	22.1 (27.14)	23.7 (28.89)	1
Lingual	88.4 (51.39)	51.4 (48.29)	<.001	26.3 (13.8)	22.1 (20.55)	1
Medial orbitofrontal	231.2 (286.15)	140.3 (163.01)	1	162.2 (149.52)	196.3 (287.72)	1
Middle temporal	41.8 (44.8)	24.3 (24.95)	1	6.2 (4.75)	4.8 (3.76)	1
Pars orbitalis	98.7 (185.26)	63.8 (120.41)	1	12.8 (13.25)	19.8 (40.29)	1
Pars triangularis	13.1 (25.08)	7.8 (17.65)	.5	4.6 (3.23)	5.1 (7.68)	1
Pericalcarine	243.2 (138.85)	142.5 (110.45)	<.001	46.6 (30.72)	40.4 (43.98)	.5
Postcentral	37.4 (27.3)	22.8 (18.07)	.55	18.8 (11.33)	14.3 (16.04)	.15
Precentral	19.8 (12.44)	11.2 (10.29)	<.001	14.8 (8.03)	8.7 (8.77)	<.001
Precuneus	84.1 (53.04)	50.2 (42.15)	<.001	35.8 (15.42)	26.3 (27.87)	<.001
Rostral middle frontal	73.3 (95.64)	51.2 (49.26)	1	13 (10.47)	15.1 (19.56)	1
Superior frontal	36.2 (27.67)	32.6 (42.06)	1	16.3 (11.66)	14.6 (18.53)	1
Superior parietal	119.1 (60.57)	74.4 (52.68)	<.001	49.8 (22.88)	44.1 (55.74)	<.001
Superior temporal	29.8 (19.49)	20.2 (18.03)	.45	9.6 (8.88)	7.1 (6.93)	1
Supramarginal	7.4 (6.04)	5.6 (4.6)	1	4.7 (3.12)	3.8 (4.06)	1

Note: Values are the connectivity measure calculated using Equation (1).

Abbreviation: MI, massa intermedia.

^aBonferroni corrected *p* values.

4 | DISCUSSION

This study is the first attempt at identifying the extent of structural connectivity of MI in the human brain. The results provide strong evidence that MI is a general commissural conduit similar to the AC and PC as well as corpus callosum, with a wide cortical and subcortical fiber distribution. The results provide further corroboration to prior work identifying fiber pathways through the MI and anterior thalamic radiation with termination in the prefrontal areas (Damle et al., 2017; Kamali et al., 2010; Kochanski et al., 2018; Spalletta et al., 2013).

A key challenge to studying MI using *in vivo* techniques such as MRI is its identification on acquired images (Nopoulos et al., 2001; Shimizu et al., 2008; Takahashi, Suzuki, Zhou, et al., 2008; Trzesniak et al., 2011). The exact prevalence of MI in the normal human population and its incidence at various decades of life remains a topic of discussion. Prior reports have noted absence of MI in 2.3–30% of normal

human brains. A recent study (Damle et al., 2017) using high resolution coronal MRI sequences found the absence of MI in 4.7% of 233 normal brains imaged. This is lower than our cohort of 12.2% which employed a similar methodology of using independent reviewers and strict criteria for identifying the MI. On the other hand, an extensive cadaveric study of 921 cases (Rabl, 1958) showed 31.7% absence of MI in different age groups. Several explanations exist for the inconsistency in the literature. MRI studies with variable signal acquisition methodologies have been used in the majority of prior studies to identify and study the MI. We used the HCP database in this study because it uses a very stringent acquisition protocol on a customized 3T MR machine with prior published quality assessment results in a pilot study. HCP provides 0.7 mm isotropic resolution images on T1W scans enabling accurate visualization of MI. We have also noted difficulty in identifying MI in younger subjects with narrow third ventricles and “kissing” thalami that cannot be differentiated

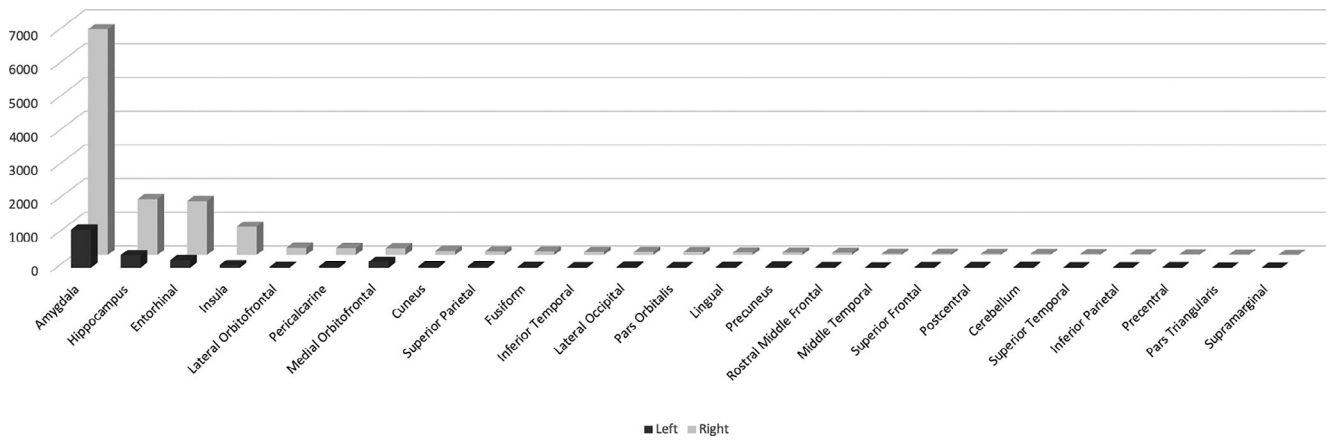


FIGURE 3 Histograms demonstrating identified gray matter (GM) targets. GM target regions are sorted from the highest to lowest based on the calculated connectivity measure using Equation (1)

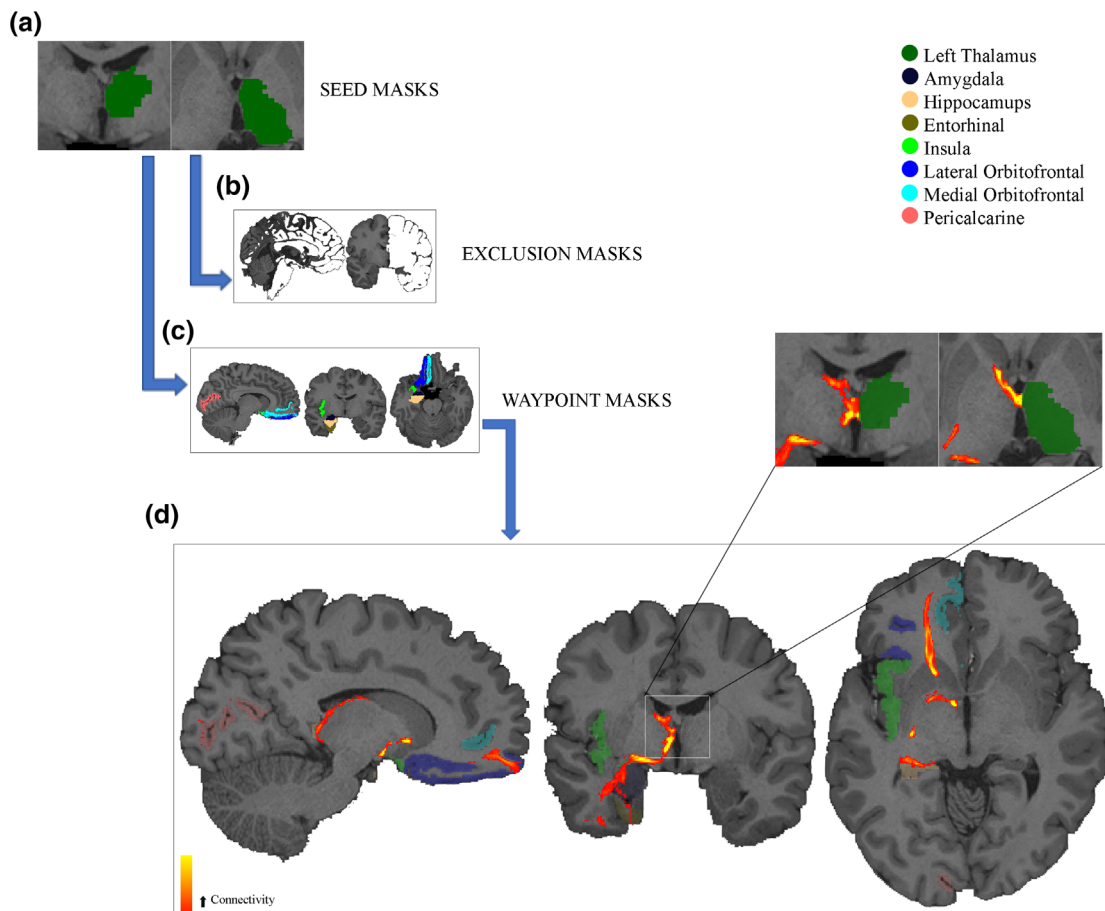


FIGURE 4 Stepwise synthesis of tractograms demonstrating existence of fibers that traverse midline through massa intermedia (MI). The ipsilateral thalamus is masked (dark green) in (a). Next, the remainder of the same hemisphere and corpus callosum, anterior and posterior commissures and brainstem are excluded (depicted in white) as shown in (b). Then contralateral waypoint masks were placed as shown in (c), in the amygdala, hippocampus, entorhinal cortex, insula, lateral and medial orbitofrontal cortices, and pericalcarine cortices. (d) shows the probabilistic map tractography between the left thalamus and right hemisphere. Crossing fibers are seen traversing via MI to the contralateral hemisphere in the *inset*

from a true MI even when multiple plane thin cut MRI sequences are obtained. Furthermore, cadaveric studies tend to be skewed toward an older population while neuroimaging studies generally employ a wider age range. While some previous reports (Damle et al., 2017; Trzesniak et al., 2011) as well as our cohort have not revealed a decline in prevalence of MI across age, these studies are uniformly limited by employing subjects with a limited range of age. On the other hand, Rabl et al., Rosales et al., and Trzesniak et al. have shown a decrease in MI presence with age (Rabl, 1958; Rosales, Lemay, & Yakovlev, 1968; Trzesniak et al., 2016). Rosales et al. have hypothesized the mechanism of “MI involution” by age (Rabl, 1958; Rosales et al., 1968; Trzesniak et al., 2016). Thus, it remains plausible that age plays a role in MI prevalence and a comprehensive longitudinal study across all decades of life is needed to identify the true prevalence of MI in the human brain.

The dorsomedial (DM) thalamic nucleus is the immediate medial GM in the thalamus through which the MI fibers may travel (Kochanski et al., 2018; Walker, 1940). Zhou et al. (2003) have reported connections between the DM thalamus and frontal cortex by way of the anterior thalamic radiation and Kamali et al. (2010) have demonstrated visualization of the anterior thalamic radiation using deterministic tractography techniques. Less clear, however, is whether the visualized DM thalamus—anterior thalamic radiation—frontal lobe pathway originates in the DM thalamus, represents *en passant* fibers of MI, or both. Shimizu et al. (2008) reported no significant correlation between DM thalamus volumes and MI volumes in a cohort of 44 healthy volunteers. More recently, Damle et al. reported an association between MI size and anterior thalamic white matter integrity among 104 healthy females. They also reported MI size differences as a mediator of outcomes in measures of attention functioning in relation to age in healthy females (Damle et al., 2017). This suggests that MI's contribution to the anterior thalamic radiation and cognitive behavior may be independent of DM thalamus. Recent work by our group demonstrating contralateral passage of stria medullaris fibers between the prefrontal cortex and habenula via the MI further supports this idea (Kochanski et al., 2018). The present study further supports the MI–frontal lobe connectivity as a strong connection between MI and lateral orbitofrontal region was noted. We also noted connectivity with the rostral middle frontal gyrus also referred to as the dorsolateral prefrontal cortex, medial orbitofrontal region, pars orbitalis, and superior frontal region. Thus, it appears that MI may be a conduit for broad frontal lobe interhemispheric connectivity. As seen in Figure 3, number of streamlines between MI and GM regions dramatically decrease in non-limbic regions, suggesting MI's primary role is interconnecting the limbic networks. A prior study in the cat model of limbic epilepsy revealed lesions placed in MI reduced interhemispheric transmission of epileptic signals, suggesting that at least in lower mammals, limbic structures such as amygdala and hippocampus communicated through MI (Hiyoshi & Wada, 1988b).

Stronger connectivity measures between MI and lateral orbitofrontal cortex in the right hemisphere (Figure 3 and Table 2) were noted in females. This may be explained by females having on average a larger MI (Borghei et al., 2020; Pavlović et al., 2020) and

larger right orbitofrontal cortices (Welborn et al., 2009). In addition, Damle et al. (2017) and Borghei et al. (2020) have reported stronger attention scores in females with MI.

The link between the absence or size of MI and psychiatric disorders, in particular SSD has been extensively reported in the literature (Nopoulos et al., 2001; Shimizu et al., 2008; Snyder et al., 1998; Takahashi, Suzuki, Zhou, et al., 2008; Zhou et al., 2003). Snyder (Snyder et al., 1998) reported that MI was absent in 34.15% of patients admitted for the first episode of psychosis due to schizophrenia as compared to 13.46% of healthy controls. Takahashi et al. reported that the relative size of amygdala in patients without MI was 0.061 in the left and 0.066 in the right hemisphere which were significantly smaller than those of schizophrenic patients with MI with relative size of 0.068 and 0.072 in the left and right hemisphere, respectively (Takahashi et al., 2008). More recent work (Aine et al., 2017; DeRosse et al., 2014; Kunimatsu et al., 2012) evaluating connectivity and diffusivity in the SSD population have demonstrated significantly lower FA values in the uncinate fasciculus of SSD patients in comparison to normal controls. In the presented study, we noted MI–amygdala connectivity by way of the uncinate fasciculus having the strongest connection to MI both in the right and left hemispheres. While these findings are preliminary, they suggest MI's main role is connecting the left and right hemispheric limbic networks. This in turn suggests lack of MI may be an independent risk factor for limbic mediated psychiatric conditions.

Demonstration of MI fibers connecting the mesial temporal lobe structures in the current study lend credence to the possible role of MI in propagation of interhemispheric epileptiform activity (Chaudhary et al., 2016; Liao et al., 2011). Lesioning experiments in the cat epilepsy model have demonstrated the role of MI in transhemispheric ictal transmission between bilateral motor cortices (Hiyoshi & Wada, 1988a, 1988b). Hiyoshi and Wada (1988b) reported that MI-lesioned cats showed a decrease in the transhemispheric positive transfer effect, requiring significantly greater stimulation for seizure propagation. Similarly, unilateral kindling resulted in gradual seizure propagation, in contrast to the abrupt generalization found in controls. In another study by Hirayasu et al. involving the rodent model, clinical manifestation of MI kindling was found to be similar to that of limbic kindling (Hirayasu & Wada, 1992b). Moreover, injection of *N*-methyl-*D*-aspartic acid into the MI of rodents led to generalized tonic-clonic seizures with continuous EEG seizure discharges in bilateral mesial temporal lobe structures (Hirayasu & Wada, 1992a). Identification of the role of MI in pathophysiology of temporal lobe epilepsy is beyond the scope of this study, but the results support prior work in lower mammals demonstrating the role of MI in interhemispheric connectivity of various mesial temporal as well as neocortical temporal lobe structures.

The significance of additional MI commissural fibers interconnecting the parietal, occipital, insular, and cerebellar regions is unclear as there are no prior studies elucidating putative clinical correlations. Such a wide distribution of interhemispheric fibers through MI is a curious finding since as noted this structure is conspicuously absent in 25–30% of the population (Nieuwenhuys, Voogd, & Van

Huijzen, 2007). It is plausible that there exists a net difference, albeit small, between the neurocognitive inventory of individuals with and without MI which may render the group without MI more susceptible to phenotypic manifestation of certain neuropsychiatric disorders. It is also plausible that individuals without MI have compensatory fiber pathways through other midline commissures resulting in no significant net neurocognitive or clinical difference. Given the accumulation of correlative literature linking psychiatric conditions to the absence of MI and the more recent objective neuropsychological measures demonstrating differences in individuals with and without MI, the former hypothesis is more likely.

There are several limitations in this study. *in vivo* imaging and post-processing are prone to errors despite meticulously designed algorithms. Errors can range from head motion to preprocessing and tractography computation methodology based on DW sequences. We attempted to mitigate this by using the HCP diffusion protocol, which uses multi-band excitation with multiple receiver to perform multi-slice EPI. This method decreases scan time and henceforth reduces head motion errors. However, despite these efforts, identification of MI was not feasible in some cases due to partial volume effects particularly in those with a narrow third ventricle, resulting in exclusion of some samples. Also, a larger number of subjects with MI included in the final analysis were female. While this was not by design, it is important to note this distinction as it may have resulted in skewness of data. Thus, results regarding MI and sexual dimorphism should be viewed in light of these limitations. Another limitation of the study was the relative homogeneity of the subjects' age range. It has been previously postulated that MI size and presence may be related to age (Rosales et al., 1968). If future studies corroborate this hypothesis, then extrapolation of our data to various age groups may be limited. Lastly, the authors acknowledge that ultimately a human neuroanatomical study employing fiber dissection and neuroanatomical staining techniques is needed to definitively elucidate the distribution of MI commissural fibers.

5 | CONCLUSION

Fibers crossing through MI have wide ranging terminations with a strong predilection for limbic structures including the mesial temporal, insula, pericalcarine and prefrontal regions. Definitive neuroanatomical studies are needed to confirm these findings.

ACKNOWLEDGMENTS

Data were provided in part by the Human Connectome Project, WU-Minn Consortium (Principal Investigators: David Van Essen and Kamil Ugurbil; 1U54MH091657) funded by the 16 NIH Institutes and Centers that support the NIH Blueprint for Neuroscience Research; and by the McDonnell Center for Systems Neuroscience at Washington University.

DATA AVAILABILITY STATEMENT

The data that support the findings of this study are openly available in Human Connectome Project at <https://db.humanconnectome.org/>

app/template/Login.vm;jsessionid=62C68CAC9F3D00C447309FFBDD8B42BA.

ORCID

Sepehr Sani  <https://orcid.org/0000-0002-1737-5269>

REFERENCES

- Aine, C., Bockholt, H., Bustillo, J., Canive, J., Caprihan, A., Gasparovic, C., ... Lauriello, J. (2017). Multimodal neuroimaging in schizophrenia: Description and dissemination. *Neuroinformatics*, 15(4), 343–364.
- Allen, L. S., & Gorski, R. A. (1991). Sexual dimorphism of the anterior commissure and massa intermedia of the human brain. *The Journal of Comparative Neurology*, 312(1), 97–104. <https://doi.org/10.1002/cne.903120108>
- Andersson, J., Xu, J., Yacoub, E., Auerbach, E., Moeller, S., & Ugurbil, K. (2012). A comprehensive Gaussian process framework for correcting distortions and movements in diffusion images. Paper presented at the Proceedings of the 20th Annual Meeting of ISMRM, Melbourne, Australia.
- Andersson, J. L., Skare, S., & Ashburner, J. (2003). How to correct susceptibility distortions in spin-echo echo-planar images: Application to diffusion tensor imaging. *NeuroImage*, 20(2), 870–888.
- Behrens, T. E., Berg, H. J., Jbabdi, S., Rushworth, M. F., & Woolrich, M. W. (2007). Probabilistic diffusion tractography with multiple fibre orientations: What can we gain? *NeuroImage*, 34(1), 144–155.
- Behrens, T. E., Woolrich, M. W., Jenkinson, M., Johansen-Berg, H., Nunes, R. G., Clare, S., ... Smith, S. M. (2003). Characterization and propagation of uncertainty in diffusion-weighted MR imaging. *Magnetic Resonance in Medicine*, 50(5), 1077–1088.
- Borghei, A., Cothran, T., Brahimaj, B., & Sani, S. (2020). Role of massa intermedia in human neurocognitive processing. *Brain Structure and Function*, 225, 985–993.
- Carpenter, M. B., & Sutin, J. (1983). *Human neuroanatomy*, Baltimore, MD: Williams & Wilkins.
- Ceyhan, M., Adapinar, B., Aksaray, G., Ozdemir, F., & Colak, E. (2008). Absence and size of massa intermedia in patients with schizophrenia and bipolar disorder. *Acta Neuropsychiatrica*, 20(4), 193–198. <https://doi.org/10.1111/j.1601-5215.2008.00296.x>
- Chaudhary, U. J., Centeno, M., Thornton, R. C., Rodionov, R., Vulliamoz, S., McEvoy, A. W., ... Carmichael, D. W. (2016). Mapping human preictal and ictal haemodynamic networks using simultaneous intracranial EEG-fMRI. *NeuroImage: Clinical*, 11, 486–493.
- Cheramy, A., Romo, R., Godeheu, G., & Glowinski, J. (1984). Effects of electrical stimulation of various midline thalamic nuclei on the bilateral release of dopamine from dendrites and nerve terminals of neurons in the nigro-striatal dopaminergic pathways. *Neuroscience Letters*, 44(2), 193–198.
- Clark, W. L. G., & Russell, W. R. (1939). Observations on the efferent connexions of the Centre median nucleus. *Journal of Anatomy*, 73(Pt. 2), 255.
- Damle, N. R., Ikuta, T., John, M., Peters, B. D., DeRosse, P., Malhotra, A. K., & Szeszko, P. R. (2017). Relationship among interthalamic adhesion size, thalamic anatomy and neuropsychological functions in healthy volunteers. *Brain Structure & Function*, 222(5), 2183–2192. <https://doi.org/10.1007/s00429-016-1334-6>
- de Macedo, F. F. (1889). De l'encéphale humain avec et sans commissure grise: essai synthétique d'observations anatomo-psychiques post mortem, et leurs relations avec la criminalité.
- DeRosse, P., Nitzburg, G. C., Ikuta, T., Peters, B. D., Malhotra, A. K., & Szeszko, P. R. (2014). Evidence from structural and diffusion tensor imaging for frontotemporal deficits in psychometric schizotypy. *Schizophrenia Bulletin*, 41(1), 104–114.
- Edinger, L. (1904). *Vorlesungen über den Bau der nervösen Zentralorgane des Menschen und der Tiere* (Vol. 1), Leipzig, Germany: Vogel.

- Fleiss, J. L., & Cohen, J. (1973). The equivalence of weighted kappa and the intraclass correlation coefficient as measures of reliability. *Educational and Psychological Measurement*, 33(3), 613–619.
- Fortuyn, J. D., & Stefens, R. (1951). On the anatomical relations of the intralaminar and midline cells of the thalamus. *Electroencephalography and Clinical Neurophysiology*, 3(4), 393–400.
- Frauceiger, E. (1959). *Neuropathologie comparée des malformations cérébrales. Malformations Congénitales du Cerveau* (pp. 41–55). Paris, France: Masson & Cie.
- Glasser, M. F., Sotiropoulos, S. N., Wilson, J. A., Coalson, T. S., Fischl, B., Andersson, J. L., ... Polimeni, J. R. (2013). The minimal preprocessing pipelines for the Human Connectome Project. *NeuroImage*, 80, 105–124.
- Grace, A. A. (2016). Dysregulation of the dopamine system in the pathophysiology of schizophrenia and depression. *Nature Reviews Neuroscience*, 17(8), 524–532.
- Hirayasu, Y., & Wada, J. A. (1992a). Convulsive seizures in rats induced by N-methyl-D-aspartate injection into the massa intermedia. *Brain Research*, 577(1), 36–40.
- Hirayasu, Y., & Wada, J. A. (1992b). N-methyl-D-aspartate injection into the massa intermedia facilitates development of limbic kindling in rats. *Epilepsia*, 33(6), 965–970.
- Hiyoshi, T., & Wada, J. A. (1988a). Midline thalamic lesion and feline amygdaloid kindling. I. Effect of lesion placement prior to kindling. *Electroencephalography and Clinical Neurophysiology*, 70(4), 325–338.
- Hiyoshi, T., & Wada, J. A. (1988b). Midline thalamic lesion and feline amygdaloid kindling. II. Effect of lesion placement upon completion of primary site kindling. *Electroencephalography and Clinical Neurophysiology*, 70(4), 339–349.
- Jin, C., Kalimo, H., & Panula, P. (2002). The histaminergic system in human thalamus: Correlation of innervation to receptor expression. *European Journal of Neuroscience*, 15(7), 1125–1138.
- Kamali, A., Kramer, L. A., & Hasan, K. M. (2010). Feasibility of prefronto-caudate pathway tractography using high resolution diffusion tensor tractography data at 3 T. *Journal of Neuroscience Methods*, 191(2), 249–254.
- Kochanski, R. B., Dawe, R., Kocak, M., & Sani, S. (2018). Identification of stria medullaris fibers in the massa intermedia using diffusion tensor imaging. *World Neurosurgery*, 112, e497–e504. <https://doi.org/10.1016/j.wneu.2018.01.066>
- Kunimatsu, N., Aoki, S., Kunimatsu, A., Abe, O., Yamada, H., Masutani, Y., ... Ohtomo, K. (2012). Tract-specific analysis of white matter integrity disruption in schizophrenia. *Psychiatry Research: Neuroimaging*, 201(2), 136–143.
- Liao, W., Zhang, Z., Pan, Z., Mantini, D., Ding, J., Duan, X., ... Lu, G. (2011). Default mode network abnormalities in mesial temporal lobe epilepsy: A study combining fMRI and DTI. *Human Brain Mapping*, 32(6), 883–895.
- Malobabic, S., Puskas, L., & Blagotic, M. (1987). Size and position of the human adhaesio interthalamica. *Gegenbaurs Morphologisches Jahrbuch*, 133(1), 175–180.
- Malobabic, S., Puskas, L., & Vujaskovic, G. (1990). Golgi morphology of the neurons in frontal sections of human interthalamica adhesion. *Acta Anatomica (Basel)*, 139(3), 234–238.
- Matsumoto, K. (1937). Über die Morphologie der massa intermedia beim Menschenhirn. *Japanese Journal of Medical Science (Anatomy)*, 6, 234.
- Mohammadi, M. R., Hosseini, S. H., & Ghalipour, M. J. (2008). Morphometric measurements of the thalamus and interthalamica adhesion by MRI in the South-East of the Caspian Sea border. *Neurosciences (Riyadh)*, 13(3), 272–275.
- Morel, A., Magnin, M., & Jeanmonod, D. (1997). Multiarchitectonic and stereotactic atlas of the human thalamus. *Journal of Comparative Neurology*, 387(4), 588–630.
- Morel, F. (1947). La massa intermedia ou commissure grise. *Cells, Tissues, Organs*, 4(1–2), 203–207.
- Nieuwenhuys, R., Voogd, J., & Van Huijzen, C. (2007). *The human central nervous system: A synopsis and atlas*, Heidelberg, Germany: Springer Science & Business Media.
- Nopoulos, P. C., Rideout, D., Crespo-Facorro, B., & Andreasen, N. C. (2001). Sex differences in the absence of massa intermedia in patients with schizophrenia versus healthy controls. *Schizophrenia Research*, 48(2–3), 177–185.
- Olry, R., & Haines, D. E. (2005). Interthalamica adhesion: Scruples about calling a spade a spade? *Journal of the History of the Neurosciences*, 14(2), 116–118. <https://doi.org/10.1080/096470490910128>
- Pavlović, M. N., Jovanović, I. D., Ugrenović, S. Z., Kostić, A. V., Kundalić, B. K., Stojanović, V. R., ... Antić, M. M. (2020). Position and size of massa intermedia in Serbian brains. *Folia Morphologica*, 79(1), 21–27. <https://doi.org/10.5603/FM.a2019.0046>
- Poretti, A., Meoded, A., Rossi, A., Raybaud, C., & Huisman, T. A. (2013). Diffusion tensor imaging and fiber tractography in brain malformations. *Pediatric Radiology*, 43(1), 28–54.
- Rabl, R. (1958). Strukturstudien an der Massa intermedia des thalamus opticus. *Journal für Hirnforschung*, 4, 78–112.
- Rioch, D. M. (1931). A note on the Centre median nucleus of Luys. *Journal of Anatomy*, 65(Pt 3), 324–327.
- Romo, R., Cheramy, A., Godeheu, G., & Glowinski, J. (1984). Distinct commissural pathways are involved in the enhanced release of dopamine induced in the contralateral caudate nucleus and substantia nigra by unilateral application of GABA in the cat thalamic motor nuclei. *Brain Research*, 308(1), 43–52.
- Rosales, R. K., Lemay, M. J., & Yakovlev, P. I. (1968). The development and involution of massa intermedia with regard to age and sex. *Journal of Neuropathology and Experimental Neurology*, 27(1), 166.
- Samra, K. A., & Cooper, I. S. (1968). Radiology of the massa intermedia. *Radiology*, 91(6), 1124–1128.
- Sen, F., Ulubay, H., Ozeksi, P., Sargon, M. F., & Tascioglu, A. B. (2005). Morphometric measurements of the thalamus and interthalamica adhesion by MR imaging. *Neuroanatomy*, 4, 10–12.
- Shimizu, M., Fujiwara, H., Hirao, K., Namiki, C., Fukuyama, H., Hayashi, T., & Murai, T. (2008). Structural abnormalities of the adhaesio interthalamica and mediodorsal nuclei of the thalamus in schizophrenia. *Schizophrenia Research*, 101(1–3), 331–338.
- Snyder, P. J., Bogerts, B., Wu, H., Bilder, R. M., Deoras, K. S., & Lieberman, J. A. (1998). Absence of the adhaesio interthalamica as a marker of early developmental neuropathology in schizophrenia: An MRI and postmortem histologic study. *Journal of Neuroimaging*, 8(3), 159–163.
- Sotiropoulos, S. N., Jbabdi, S., Xu, J., Andersson, J. L., Moeller, S., Auerbach, E. J., ... Jenkinson, M. (2013). Advances in diffusion MRI acquisition and processing in the Human Connectome Project. *NeuroImage*, 80, 125–143.
- Spalletta, G., Fagioli, S., Caltagirone, C., & Piras, F. (2013). Brain microstructure of subclinical apathy phenomenology in healthy individuals. *Human Brain Mapping*, 34(12), 3193–3203.
- Takahashi, T., Suzuki, M., Nakamura, K., Tanino, R., Zhou, S.-Y., Hagino, H., ... Kurachi, M. (2008). Association between absence of the adhaesio interthalamica and amygdala volume in schizophrenia. *Psychiatry Research: Neuroimaging*, 162(2), 101–111.
- Takahashi, T., Suzuki, M., Zhou, S.-Y., Nakamura, K., Tanino, R., Kawasaki, Y., ... Kurachi, M. (2008). Prevalence and length of the adhaesio interthalamica in schizophrenia spectrum disorders. *Psychiatry Research: Neuroimaging*, 164(1), 90–94.
- Trzesniak, C., Kempton, M. J., Busatto, G. F., de Oliveira, I. R., Galvao-de Almeida, A., Kambitz, J., ... Crippa, J. A. (2011). Adhaesio interthalamica alterations in schizophrenia spectrum disorders: A systematic review and meta-analysis. *Progress in Neuro-Psychopharmacology & Biological Psychiatry*, 35(4), 877–886. <https://doi.org/10.1016/j.pnpbp.2010.12.024>

- Trzesniak, C., Linares, I. M., Coimbra, E. R., Junior, A. V., Velasco, T. R., Santos, A. C., ... Crippa, J. A. (2016). Adhesio interthalamica and cavum septum pellucidum in mesial temporal lobe epilepsy. *Brain Imaging and Behavior*, 10(3), 849–856. <https://doi.org/10.1007/s11682-015-9461-x>
- Van Essen, D. C., Smith, S. M., Barch, D. M., Behrens, T. E., Yacoub, E., Ugurbil, K., & Consortium, W.-M. H. (2013). The WU-Minn human connectome project: An overview. *NeuroImage*, 80, 62–79.
- Van Essen, D. C., Ugurbil, K., Auerbach, E., Barch, D., Behrens, T., Bucholz, R., ... Curtiss, S. W. (2012). The Human Connectome Project: A data acquisition perspective. *Neuroimage*, 62(4), 2222–2231.
- Wada, J. A., Sato, M., & Corcoran, M. E. (1974). Persistent seizure susceptibility and recurrent spontaneous seizures in kindled cats. *Epilepsia*, 15(4), 465–478.
- Walker, A. E. (1940). The medial thalamic nucleus. A comparative anatomical, physiological and clinical study of the nucleus medialis dorsalis thalami. *Journal of Comparative Neurology*, 73(1), 87–115.
- Welborn, B. L., Papademetris, X., Reis, D. L., Rajeevan, N., Bloise, S. M., & Gray, J. R. (2009). Variation in orbitofrontal cortex volume: Relation to sex, emotion regulation and affect. *Social Cognitive and Affective Neuroscience*, 4(4), 328–339.
- Zhou, S.-Y., Suzuki, M., Hagino, H., Takahashi, T., Kawasaki, Y., Nohara, S., ... Kurachi, M. (2003). Decreased volume and increased asymmetry of the anterior limb of the internal capsule in patients with schizophrenia. *Biological Psychiatry*, 54(4), 427–436.

SUPPORTING INFORMATION

Additional supporting information may be found online in the Supporting Information section at the end of this article.

How to cite this article: Borghei A, Kapucu I, Dawe R, Kocak M, Sani S. Structural connectivity of the human massa intermedia: A probabilistic tractography study. *Hum Brain Mapp*. 2021;42:1794–1804. <https://doi.org/10.1002/hbm.25329>